Self-Assembly of 1,4-Benzenedithiolate/Tetrahydrofuran on a Gold Surface: A Monte Carlo Simulation Study

Xiongce Zhao,*,† Yongsheng Leng,‡ and Peter T. Cummings†,‡

Nanomaterials Theory Institute, Center for Nanophase Materials Sciences, Oak Ridge National Laboratory, Oak Ridge, Tennessee 37831, and Department of Chemical Engineering, Vanderbilt University, Nashville, Tennessee 37235

Received November 29, 2005. In Final Form: February 21, 2006

We report a Monte Carlo simulation study of the self-assembly of 1,4-benzenedithiolate (BDT), tetrahydrofuran (THF), and their mixtures on a Au (111) surface. We use the grand canonical Monte Carlo method to obtain the equilibrium adsorption coverage. Canonical ensemble (*NVT*) simulation is then used to explore further the structural information of the equilibrated systems. Our results indicate that BDT molecules adsorb onto the Au (111) surface with one of the sulfur atoms bonded to Au atoms. THF molecules form clusters on the surface. For BDT−THF mixtures, BDT can selectively adsorb on Au (111) to form a monolayer, whereas the solvent THF molecules either float above BDT monolayer or occupy vacancies on the surface that are not covered by BDT molecules. BDT molecules adsorb on a Au (111) surface with an average tilt angle of about 18−35° to the surface normal. The tilting angle decreases as the coverage increases. In addition, the BDT monolayer constitutes an ordered herringbone structure on the Au (111) surface, and the ordering pattern is insensitive to the BDT coverage. In comparison, the THF molecules exhibit amorphous structure on the Au surface. Interestingly, simulations indicate that the bonding behavior of BDT molecules on Au (111) is coverage-dependent. BDT bonds preferably on the Au top site when the surface coverage is low. As coverage increases, most BDT molecules bond on the bridge and fcc hollow sites.

I. Introduction

One of the most important applications of surface self-assembled monolayers[1] (SAMs) by organic molecules is in molecular electronics.[2] Early in the 1970s, Aviram and Ratner proposed that certain organic molecules may be used to construct electronic devices.[3] Extensive experimental and theoretical work has been performed in recent years on probing such a possibility. It has been demonstrated that some of the thiolate molecules, such as 1,4-benzenedithiolate (BDT), show promising conducting properties when they are assembled on gold tips. Current−voltage and conductance properties of BDT molecular junctions have been measured experimentally by several independent groups.[4−6] Theoretical approaches have been mainly focused on reproducing the current−voltage behavior observed in experiments using electronic simulations. Examples of such calculations are the density-functional-theory-based simulations of the conductance of BDT/Au systems.[7−11] These simulations qualitatively reproduced the characteristics of the current−voltage curve from experiments but showed large deviations quantitatively. One possible reason is insufficient information as input in order for ab initio calculations to yield accurate results. Such needed information includes the conformation, bonding properties, and actual adsorption conditions of the Au−BDT−Au junctions.[12−16] Some of these properties can be obtained via classical molecular dynamics or Monte Carlo simulations.[17] A better understanding of the details occurring during self-assembly adsorption through classical simulations can provide better input information for future ab initio calculations. Classical modeling also helps in interpretation and gives useful feedback pertaining to the experimental measurements and device design and manufacture. Therefore, classical molecular simulations of SAMs constitute an important intermediate step toward understanding fundamental issues related to molecular electronics devices.

In this article, we report grand canonical and canonical ensemble Monte Carlo simulations of BDT/tetrahydrofuran (THF) and their mixture adsorption on Au (111) surfaces. This work follows our previous theoretical studies[11,18,19] on molecular electronics devices made of Au and BDT molecules. In previous work, we have performed a molecular dynamics (MD) study of BDT bonded to a Au (111) surface[18] and tested the Au−BDT interaction potentials by comparing the equilibrated structure of a defect-free BDT monolayer with available experimental results. In this work, we concentrate on the adsorption process, surface conformation, and ordering of BDT on Au (111) surfaces. The results presented here differ from our previous work in two

* To whom correspondence should be addressed. E-mail: zhaox@ornl.gov.
† Oak Ridge National Laboratory.
‡ Vanderbilt University.

(1) Schreiber, F. *J. Phys.: Condens. Matter* **2004**, *16*, R881.
(2) McCreery, R. L. *Chem. Mater.* **2004**, *16*, 4477.
(3) Aviram, A.; Ratner, M. A. *Chem. Phys. Lett.* **1974**, *29*, 277.
(4) Reed, M. A.; Zhou, C.; Muller, C. J.; Burgin, T. P.; Tour, J. M. *Science* **1997**, *278*, 252.
(5) Xu, B. Q.; Tao, N. J. *Science* **2003**, *301*, 1221.
(6) Blum, A. S.; Kushmerick, J. G.; Long, D. P.; Patteson, C. H.; Yang, J. C.; Henderson, J. C.; Yao, Y. X.; Tour, J. M.; Shashidhar, R.; Ratna, B. R. *Nat. Mater.* **2005**, *4*, 167.
(7) Seminario, J. M.; Zacarias, A. G.; Tour, J. M. *J. Phys. Chem. A* **1999**, *103*, 7883.
(8) Di Ventra, M.; Pantelides, S. T.; Lang, N. D. *Phys. Rev. Lett.* **2000**, *84*, 979.
(9) Kornilovitch, P. E.; Bratkovsky, A. M. *Phys. Rev. B* **2001**, *64*, 195413.
(10) Stokbro, K.; Talyor, J.; Brandbyge, M.; Mozos, J. L.; Ordejon, P. *Comput. Mater. Sci.* **2003**, *27*, 151.
(11) Krstić, P. S.; Dean, D. J.; Zhang, X. G.; Keffer, D.; Leng, Y. S.; Cummings, P. T.; Wells, J. C. *Comput. Mater. Sci.* **2003**, *28*, 312.
(12) Joachim, C.; Gimzewski, J. K.; Aviram, A. *Nature* **2000**, *408*, 541.
(13) Chen, J.; Reed, M. A.; Rawlett, A. M.; Tour, J. M. *Science* **1999**, *286*, 1550.
(14) Di Ventra, M.; Kim, S. G.; Pantelides, S. T.; Lang, N. D. *Phys. Rev. Lett.* **2001**, *86*, 288.
(15) Hipps, K. W. *Science* **2001**, *294*, 536.
(16) Yaliraki, S. N.; Kemp, M.; Ratner, M. A. *J. Am. Chem. Soc.* **1999**, *121*, 3428.
(17) Jiang S. Y. *Mol. Phys.* **2002**, *100*, 2261.
(18) Leng, Y. S.; Keffer, D. J.; Cummings, P. T. *J. Phys. Chem. B* **2003**, *107*, 11940.
(19) Leng, Y. S.; Krstić, P. S.; Wells, J. C.; Cummings, P. T.; Dean, D. J. *J. Chem. Phys.* **2005**, *122*, 244721.

10.1021/la0532252 CCC: $33.50
Published on Web 03/29/2006

ways: First, the grand canonical Monte Carlo method results in BDT SAMs that are not defect-free (and hence are closer to experimental reality). Second, part of simulation results reported here explicitly include the solvent molecules (THF) in order to mimic an adsorption environment that is as close to experimental conditions[4] as possible. Orientation-biased grand canonical Monte Carlo (GCMC) techniques are used to simulate the adsorption of BDT/THF onto a Au surface from bulk BDT/THF and their mixtures. This is followed by the canonical ensemble (*NVT*) Monte Carlo moves to equilibrate the structure of the adsorbate layers extensively. The adsorbate (BDT, THF, and mixtures) structure is collected in *NVT* simulations and analyzed.

The article is organized as follows. In section II, we give detailed descriptions of the potential models used in the simulations; in section III, we describe the simulation techniques employed in the study; and in section IV, we present the results that include the equilibrated structural information of BDT, THF, and their mixtures on Au (111). We present our conclusions in section V.

II. Potential Models

1. Bulk BDT Potential Model. The BDT molecules in the bulk are modeled by an explicit-atom potential based on the universal force field (UFF).[26] The rigid framework configuration of BDT is taken from the MD-optimized structure using the UFF potential in our previous work.[18] The optimization utilized the UFF potential which includes energy terms of bond stretching, bond angle bending, dihedral angle torsion, inversion, and nonbonded interaction (van der Waals and electrostatic) between atoms separated by more than two atoms within one molecule or between atoms in different molecules. We use the equilibrated BDT molecular configuration from the optimization as the stable, rigid BDT configuration in both bulk and adsorbed phases. A schematic of a bulk BDT molecule is shown in Figure 1.

We adopt the BDT potential we used before[18] but with some modifications. The potential of bulk BDT consists of two types of nonbonded interactions—the Lennard-Jones-type dispersion energy and electrostatic energy. The Lennard-Jones energy between a pair of interacting sites i and j located on different molecules is given by

$$U_{ij}^{\mathrm{LJ}} = 4\epsilon_{ij}\left[\left(\frac{\sigma_{ij}}{r_{ij}}\right)^{12} - \left(\frac{\sigma_{ij}}{r_{ij}}\right)^{6}\right] \qquad (1)$$

Cross-interaction potential parameters ϵ_{ij} and σ_{ij} are calculated from Lorentz−Berthelot combining rules if interacting sites i and j are different species. The Lennard-Jones parameters in eq 1 for each interacting site on BDT are converted from corresponding UFF parameters, which are same as the ones used in our previous study.[18] In this work, the partial charges of BDT are different from the ones we used in ref 18. They are derived from our recent quantum mechanical simulations[19] in which partial charges were calculated from three DFT functionals—LDA, PBE0, and X3LYP. The results based on the three functionals are very close to each other. Therefore, we use the partial charges

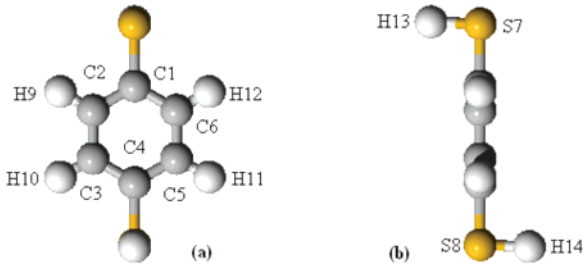

Figure 1. (a) Rigid bulk BDT molecular configuration used in the simulation. (b) Side view of a.

Table 1. Molecular Configuration and Potential Parameters for the Bulk BDT Model

Bond Lengths (Å)	
C−C (benzene ring)	1.379
C−H	1.085
C−S	1.800
S−H	1.429
Bond Angles	
C1−C2−C3	120°
C1−C2−H9	120°
C2−C1−S7	120°
C1−S7−H13	92.1°

Lennard-Jones Parameters

	ϵ (kcal/mol)	σ (Å)[a]
C	0.105	3.431
H	0.044	2.571
S	0.274	3.595

Partial Charges

	q(e)
C1, C4	−0.49
C2, C3, C5, C6	−0.06
S	0.06
H9, H10, H11, H12	0.20
H13, H14	0.15

[a] Converted from UFF parameters.

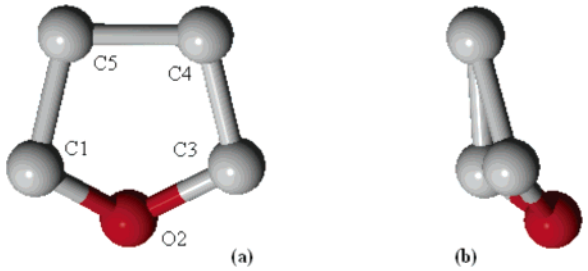

Figure 2. (a) United-atom frame of the THF model in the twist conformation. (b) Side view of a.

averaged from these three sets of results. The energies of bonds, angles, and dihedrals need not be included because we assume that the BDT molecule is rigid. The molecular configuration and potential parameters for the bulk BDT are summarized in Table 1.

2. THF Potential Model. The solvent molecule THF is modeled as a rigid united-atom ring. The THF molecule can be in one of the three configurational structures—planar, envelope, or twist. Ab initio calculations by Girard and Müller-Plathe showed that the twist configuration is the most stable one.[20] Therefore, we used the twist form of THF in all of our simulations. A schematic frame of the THF model is given in Figure 2.

Currently available potential models for THF include the

(20) Garard, S.; Müller-Plathe, F. *Mol. Phys.* **2003**, *101*, 779.
(21) Chandrasekhar, J.; Jorgensen, W. L. *J. Chem. Phys.* **1982**, *77*, 5073.
(22) Briggs, J. M.; Matsui, T.; Jorgensen, W. L. *J. Comput. Chem.* **1990**, *11*, 958.
(23) Helfrich, J.; Hentschke, R. *Macromolecules* **1995**, *25*, 3831.
(24) Faller, R.; Schmitz, H.; Biermann, O.; Müller-Plathe, F. *J. Comput. Chem.* **1999**, *20*, 1009.
(25) Damm, W.; Frontera, A.; Tirado-Rives, J.; Jorgensen, W. L. *J. Comput. Chem.* **1984**, *18*, 1955.
(26) Rappé, A. K.; Cassewit, C. J.; Colwell, K. S.; Goddard, W. A., III; Skiff, W. M. *J. Am. Chem. Soc.* **1992**, *114*, 10024.

Table 2. Molecular Configuration and Potential Parameters for the THF Model

Bond Lengths (Å)	
C−O	1.432
C−C	1.523
Bond Angles	
C1−O2−C3	109.6°
O2−C3−C4	108.0°
C3−C4−C5	101.4°

Lennard-Jones Parameters

	ϵ (kcal/mol)	σ (Å)
carbon groups	0.09	4.3
O	0.20	3.2

Partial Charges

	q(e)
C1, C3	0.28
O	−0.54
C4, C5	−0.01

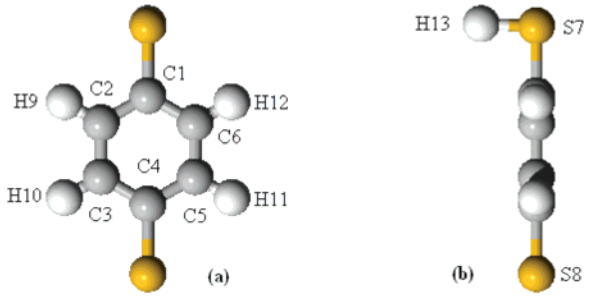

Figure 3. (a) Configuration of BDT with one H removed. The S8 atom is assumed to form chemical bonds with Au atoms. (b) Side view of a.

united-atom type[21−23] and the all-atom type.[24−27] The MD simulation results by Girard and Müller-Plathe suggest that two of united-atom models perform better than other potentials in reproducing the THF physical properties.[20] We chose the united-atom model by Helfrich and Hentschke[23] because this model performs best when used in mixture simulations.[23] In this model, Lennard-Jones and electrostatic interaction sites of THF are located on the oxygen atom and four carbon atoms, with hydrogen atoms being implicit. The THF−THF and THF−BDT Lennard-Jones interactions are treated the same way as that in modeling BDT molecules described in section II.1. The configurational information and the potential parameters of the rigid THF model are summarized in Table 2.

3. Au−BDT Potential. When a BDT molecule adsorbs on a Au (111) surface, one of the sulfur atoms will form chemical bonds with Au atoms, accompanied by the dissociation of the H atom from the originally bonded sulfur atom (Figure 3). Our ab initio calculations indicate that the configuration of the BDT molecule is largely unchanged but significant charge transfer occurs during the Au−S bonding process.[19] Therefore, to model the bonded BDT we use the same Lennard-Jones potential as used for the bulk BDT but with modified partial charges. The redistributed partial charges for the bonded BDT molecule were obtained from the average of ab initio results[19] of three DFT functionals for the bridge bonding configuration. Table 3 summarizes the partial charges for the bonded BDT model, together with the Lennard-Jones parameters for the Au atom.

One crucial choice in this work is the selection of the potential model for the chemical bonding between the S atom in BDT and the Au atoms in the substrate. We chose the pairwise additive Morse potential to describe the Au−S interaction. The Morse-type potentials had been used previously to approximate the chemical adsorption of BDT on the Au surface.[28,29] Here, the Morse potential takes the form

Table 3. Partial Charges for the Potential of Adsorbed BDT Molecules and Lennard-Jones Parameters for Au Atoms

Partial Charges

	q(e)
C1	−0.49
C2, C6	−0.06
C4	−0.33
C3, C5	−0.10
S7	0.06
S8	0.13
H9, H10, H11, H12	0.20
H13	0.15
Au	0.00

Lennard-Jones Parameters

	ϵ (kcal/mol)	σ (Å)
Au	0.039	2.935

Table 4. Potential Parameters for the Morse Au−S Bonding Interaction[29]

D_e (kcal/mol)	r_e (Å)	α (1/Å)
8.763	2.65	1.47

$$U_{\text{Morse}}^{\text{Au-S}} = D_e \exp[-\alpha(r - r_e)]\{\exp[-\alpha(r - r_e)] - 2\} \quad (2)$$

In eq 2, r is the distance between a pair of S and Au atoms, and D_e, r_e, and α are empirical parameters. In this work, we use the Morse potential parameters fitted from experiments.[29] The experimental fitted parameters[29] (Table 4) are based on the energy data from temperature-programmed desorption (TPD) of BDT on a Au (111) surface.[30,31] The suggested range of the pairwise sum of this Morse potential parametrization is $2.5r_e$.[29] There are also parameters fitted from our previous ab initio study.[19] We chose the experimentally fitted Morse potential because it is based on the isotropic interaction between each pair of Au and S atoms, whereas the ab initio fitted parameters are based on the localized interactions due to the limited numbers of atoms used in the DFT calculations. In our Monte Carlo simulations, we assume that the Morse potential is isotropic. That is, any pair of Au−S within $2.5r_e$ has a Morse interaction. Therefore, the isotropic model is a better choice in this study than the ab initio models we reported previously. However, comparison simulations of BDT/Au (111) using all of the available Morse parameters for Au−S interaction will be reported in a future paper.

III. Simulation Methodology

1. Simulation Details. We have used a grand canonical (μVT ensemble) Monte Carlo method to determine the equilibrium adsorption coverages of BDT and THF and the BDT−THF mixture on a Au surface. Canonical (NVT ensemble) Monte Carlo simulations were followed to equilibrate the structures further and to collect the orientation information of the adsorbed phase

(27) Verlinde, C. L.; De Ranter, C. J.; Blaton, N. M.; Peeters, O. M. *Acta Crystallogr., Sect. B* **1989**, *45*, 107.
(28) Sadreev, A. F.; Sukhinin, Y. V. *J. Chem. Phys.* **1997**, *107*, 2643.
(29) Mahaffy, R.; Bhatia, R.; Garrison, B. J. *J. Phys. Chem. B* **1997**, *101*, 771.
(30) Nuzzo, R. G.; Zegaarski, B. R.; Dubois, L. H. *J. Am. Chem. Soc.* **1987**, *109*, 733.
(31) Dubois, L. H.; Nuzzo, R. G. *Annu. Rev. Phys. Chem.* **1992**, *43*, 437.

with fixed coverage from GCMC. A detailed description of μVT and *NVT* Monte Carlo techniques can be found in refs 32 and 33.

The simulation cell has dimensions of $57.6 \times 49.8 \times 50$ Å^3. The rectangular Au substrate consists of three Au (111) layers with each layer consisting of 400 Au atoms. A repulsive (reflecting) wall was placed opposite to the Au (111) surface. Periodic boundary conditions are applied in the lateral x and y directions of the simulation box. All of the Au atoms are fixed during simulations.

Four kinds of Monte Carlo moves are involved in GCMC simulations: (i) translation of the center of mass of an adsorbate molecule, (ii) rotation of a molecule, (iii) insertion of a molecule, and (iv) deletion of a molecule. Because of the size and configuration complexity of the THF and BDT molecules, conventional GCMC techniques are very inefficient for inserting and deleting moves. Therefore, we implemented the orientationally biased GCMC[34] to improve the efficiency of the simulation. Each attempted insertion or deletion of a molecule utilized information from 15 random orientations.

Both GCMC and *NVT* simulations were carried out at 298 K. A typical simulation run included 2−5 million GCMC moves consisting of four types of moves attempted with equal probability of $^1/_4$. The coverage-equilibrated configuration from GCMC was input as the starting point of the *NVT* simulations. The further *NVT* equilibration typically included 5−10 million translation and rotation moves, each performed with equal probability. An additional 5 million *NVT* moves followed for collection of the structural data. The maximum values of translation and rotation of the molecules were adjusted during the equilibrations to achieve acceptance ratios for these moves of about 0.4.

The cutoff of the pairwise Lennard-Jones interaction between the interacting sites of BDT, THF, and Au atoms was 15 Å, with no long-range correction applied. In BDT/Au systems, the long-range Columbic interaction plays a critical role in determining the equilibration structures of the adsorbate phase.[18] We employed the pseudo-2-D Ewald summation technique to calculate the electrostatic interactions in the system. This method is based on a correction scheme to the conventional 3-D Ewald method.[35,36] It had been shown[18] that this 2-D Ewald method (EW3DC) is an excellent approximation to the exact 2-D (periodicity exists only in the x and y directions) Ewald method when the interacting distance between two charge sites is within 45 Å in the z direction, whereas it is computationally much faster than an exact 2-D Ewald summation. We used this method because the adsorbed phase is well localized near the Au surface and the distance in the z direction between two typical charge sites in the simulation box is less than 45 Å (the simulation box is 50 Å in z direction). The detailed description and computational algorithm of the EW3DC method can be found in our previous paper[18] and the original literature.[35,36]

2. Simulation of Au−S Bonding. At the beginning of each simulation, typically 32 BDT or THF (or 16 BDT and 16 THF for mixture simulations) molecules are arranged in an fcc lattice above the Au (111) surface. The closest distance between the adsorbate molecules and the top-layer Au atoms is greater than $2.5r_e$ to avoid direct interactions between BDT and Au through chemical bonding potentials in the initial stage. During the GCMC runs, BDT molecules are allowed to interact with the Au atoms through either Lennard-Jones or isotropic Morse potentials, depending on the distance between the S atoms in BDT and the Au surface. If neither of the S atoms in a BDT molecule is within the Morse interaction distance ($r < 2.5r_e$) of the Au surface atoms, then the energy between BDT and Au atoms is calculated by the pairwise Lennard-Jones interaction. The electrostatic energy involving the BDT molecule is calculated from the partial charges of bulk BDT. As soon as one of the S atoms of a BDT molecule is in the range of less than $2.5r_e$ from the Au surface, the Morse potential is in effect between the S atom and Au atoms. At the same time, the Lennard-Jones interaction between this S atom and Au atoms is turned off. When a S atom begins to interact with the Au surface by the Morse potential, the H atom originally bonded to it is removed and assumed not to interact with the system. The Lennard-Jones interaction between the bonded BDT and other BDT/THF molecules remains the same except that the H atom and its interactions have been removed; the electrostatic interaction due to the newly bonded BDT is calculated on the basis of the redistributed partial charges. Please note that the partial charges of a bonded BDT are no longer symmetrically distributed as are those in a bulk BDT. Physically, only one of the S atoms bonds with the Au surface when they are within the bonding distance, so we chose the one closer to the Au surface as the bonding S when both S atoms in a BDT are within the bonding distance, $2.5r_e$. If accidentally (although rarely) the distances of both S atoms of a BDT molecule to the Au surface are within $2.5r_e$ and identical to each other, then we randomly choose one of the S atoms as the bonding atom, with equal probability. We should point out that the interaction between a BDT molecule and a Au surface at a distance of $2.5r_e$ is very weak. The Morse S−Au interaction at $2.5r_e$ is less than 0.3% of its potential well depth. The LJ interaction between S−Au and H−Au at $2.5r_e$ is even weaker, less than 0.1% of the Morse potential well depth. Therefore, the total potential energy discontinuity due to turning the Morse potential on and off at $2.5r_e$ can be safely neglected.

During a GCMC simulation, the desorption and adsorption of BDT molecules on the Au surface occurs with equal rates once the system reaches equilibrium. The energy calculation of a desorbing BDT molecule can be easily performed by reversing the above schemes. When a bonding S atom detaches from the Au surface and moves out of the interacting range of the Morse potential, the H atom originally bonded to it resumes its position according to the bulk BDT configuration. The partial charges are switched back to a regular bulk BDT, the Morse interaction of the S atom is turned off, and the Lennard-Jones interactions are turned on. This association and dissociation process is conveniently realized by identity-swapping techniques utilized in simulating mixture adsorptions.[37]

IV. Results and Discussions

1. THF Adsorption on Au. An experimental study of the self-assembly of alkanethiols on a Au surface usually uses THF as a solvent.[4,38−42] It is therefore important to understand how THF interacts with a Au substrate. To our knowledge, there is no molecular simulation study of THF/Au surface systems. THF

(32) Allen, M. P.; Tildesley, D. J. *Computer Simulation of Liquids*; Oxford University Press: New York, 1987.
(33) Frenkel, D.; Smit, B. *Understanding Molecular Simulation*, 2nd ed.; Academic Press: London, 2002.
(34) Smit B. *Mol. Phys.* **1995**, *85*, 153.
(35) Yeh, I. C.; Berkowitz, M. L. *J. Chem. Phys.* **1999**, *111,* 3155.
(36) Smith, E. R. *Proc. R. Soc. London, Ser. A* **1981**, *375*, 475.
(37) Cracknell, R. F.; Nicholson, D.; Quike, N. *Mol. Simul.* **1994**, *13*, 161.
(38) Choo, H.; Cutler, E.; Shon, Y. S. *Langmuir* **2003**, *19*, 8555.
(39) Silin, V. I.; Wieder, H.; Woodward, J. T.; Valincius, G.;, Offenhausser, A.; Plant, A. L. *J. Am. Chem. Soc.* **2002**, *124*, 14676.
(40) Cai, L. T.; Yao, Y. X.; Yang, J. P.; Price, D. W.; Tour, J. M. *Chem. Mater.* **2002**, *14*, 2905.
(41) Vanderah, D. J.; Valincius, G.; Meuse, C. W. *Langmuir* **2002**, *18*, 4674.
(42) Schlenoff, J. B.; Li, M.; Ly, H. *J. Am. Chem. Soc.* **1995**, *117*, 12528.

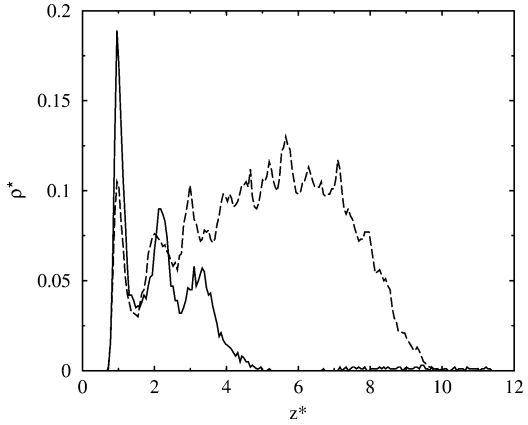

Figure 4. Local density profiles (in reduced units) of THF molecules along the normal direction of the Au (111) surface. The Au surface is at $z^* = 0$ (z^* is in reduced units). The solid line is for the adsorption coverage of $N_a = 3.36$ μmol/m^2 (2.02 molecule/nm^2), and the dashed line is for coverage $N_a = 11.58$ μmol/m^2 (6.97 molecule/nm^2).

is deemed to be a good solvent for the study of SAMs on Au because of its stable, nontoxic properties and its excellent solvation with most alkanethiolate molecules. It is known that THF does not form chemical bonds with the Au surface.

Our simulation study focuses on the adsorption pattern and the structure of physisorbed THF on Au. We found that THF molecules form clusters when they adsorb on the Au (111) surface rather than spread out to form a clean monolayer or multilayers. Such clustered structures are observed for both low and high coverages. In Figure 4, we present the density profiles of THF on Au (111) at two different coverages. We can see that under a relatively low coverage $N_a = 3.36$ μmol/m^2 (2.02 molecule/nm^2) THF molecules conform roughly to three layers on the surface but there are no distinct boundaries between layers. For a higher coverage $N_a = 11.58$ μmol/m^2 (6.97 molecule/nm^2), the adsorbed THF molecules also conform to an indistinct three-layer structure near the surface but virtually form an amorphous structure beyond (dashed line in Figure 4). It should be noted that the density profiles in Figure 4 are from one typical simulation and the quantitative details of the profiles from different runs may vary because of the inhomogeneous nature of the THF density across the surface.

The amorphous structure of THF on Au (111) can be seen more clearly if we examine the structural snapshots taken during simulations. In Figure 5, we present snapshots of THF on Au (111) under the low coverage (a) and high coverage (b) discussed above. We can see that THF molecules stick to each other above the Au (111) rather than spread uniformly on the surface. This is true even for the low-coverage simulation, where there is apparently enough space on the Au surface for THF molecules to spread out. We note that the results shown here were obtained after a very long simulation and the systems were very well equilibrated.

The wetting behavior of a fluid on a surface is determined by the relative strength between fluid−fluid interaction and fluid−surface interaction. We attribute the cluster structures of THF on Au (111) to the strong inter-THF interactions over the THF−Au interaction. In our simulations, we noticed that the electrostatic interaction between the THF molecules dominates the potential energy of the system. THF−THF interaction contributes more than 60% of the total energy on an average level. For such a strong relative adsorbate−adsorbate interaction, it is not surprising that the adsorbates would stick together to form clusters rather than spread out on the adsorbent.[43]

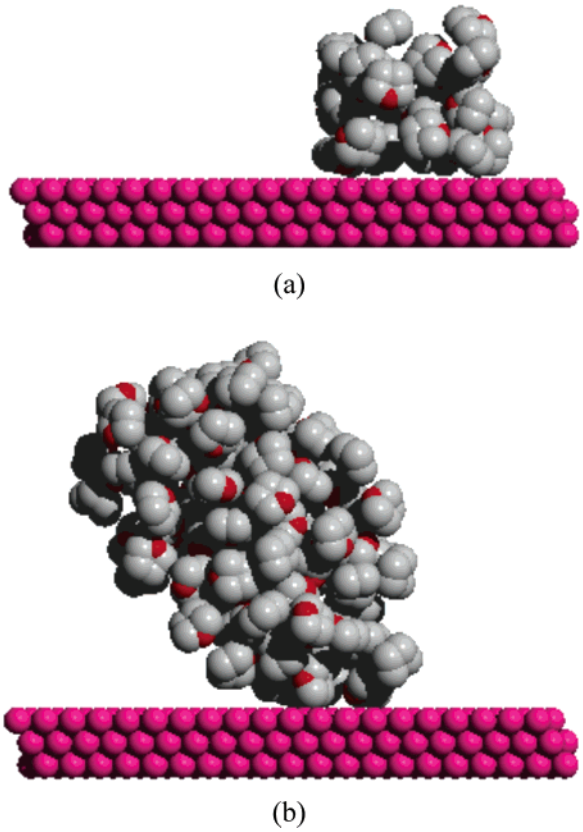

Figure 5. Snapshots of THF adsorbed on a Au (111) surface. (a) Structure of THF/Au with a coverage of $N_a = 3.36$ μmol/m^2 (2.02 molecule/nm^2). (b) Structure of THF/Au with a coverage of $N_a = 11.58$ μmol/m^2 (6.97 molecule/nm^2).

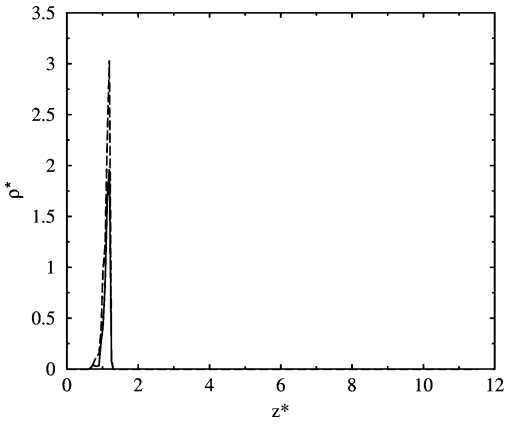

Figure 6. Local density profiles of BDT molecules along the normal direction of Au (111). The solid line is for the adsorption coverage of $N_a = 2.72$ μmol/m^2 (1.64 molecule/nm^2), and the dashed line is for coverage $N_a = 4.34$ μmol/m^2 (2.61 molecule/nm^2).

2. BDT Adsorption on Au. In Figure 6, we show the density profiles of BDT on Au (111) under two different submonolayer coverages. We found that BDT molecules form a highly ordered monolayer structure on the Au (111) surface. As can be seen, the centers of mass of adsorbed BDT are distributed very sharply around $z = 5$ Å ($z^* = 1.2$) from the gold surface. The shape of density profiles seems to be independent of coverage as long as the total number of molecules adsorbed is below a full monolayer (estimated full monolayer coverage[44] for our system is 7.08 μmol/

(43) Myers, A. L.; Calles, J. A.; Calleja, G. *Adsorption* **1999**, *3*, 107.
(44) Wan, L. J.; Terashima, M.; Noda, H.; Osawa, M. *J. Phys. Chem. B* **2000**, *104*, 3563.

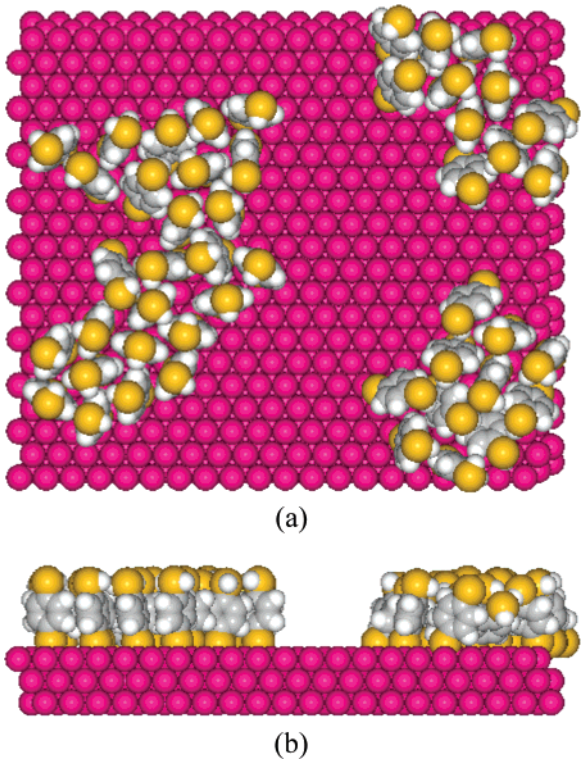

Figure 7. Snapshots of BDT adsorbed on a Au (111) surface with a coverage of $N_a = 2.72\ \mu mol/m^2$ (1.64 molecule/nm^2). (a) Top view and (b) side view.

m^2 (4.27 BDT molecule/nm^2)). This is in stark contrast to the adsorption of solvent THF molecules.

In Figures 7 and 8, we present snapshots of BDT/Au (111) from simulations. We can see that under either coverage, BDT molecules bond through one sulfur atom to the gold surface, with a tilt angle between the BDT molecular plane and the surface normal. We found that even under very low coverage, BDT molecules have a tilted angle rather than a flat orientation. Different experimental reports exist on the tilt of alkanethiolates on the Au surface.[45−47] Some experiments suggest that the tilting angle of alkanethiolates on Au does not depend on the molecular type or surface type,[47,48] and another experiment indicates that the tilting is strongly dependent on the surface coverage.[46] Our simulations indicate that the tilt angle of BDT on Au (111) depends slightly on the surface coverage, with the average tilting angle decreasing as the coverage increases. In Table 5, we give the average tilting angles between the BDT molecular plane and the Au surface normal at different submonolayer coverages. We can see that the average tilt angle decreases from around 35° to about 18° as the coverage increases from 0.64 to 6.25 μmol/m^2 (0.38 to 3.77 molecule/nm^2). This is qualitatively consistent with the experimental findings reported in the work of Joo et al.[46] and other work.[18,49,50]

We notice that the average tilting angle of BDT fluctuates significantly. (See the large standard deviation in Table 5.) This can be seen from snapshots shown in Figure 8 for the coverage of 6.25 μmol/m^2. For most of the BDT molecules, the tilt angle with respect to the surface normal is very small, whereas some

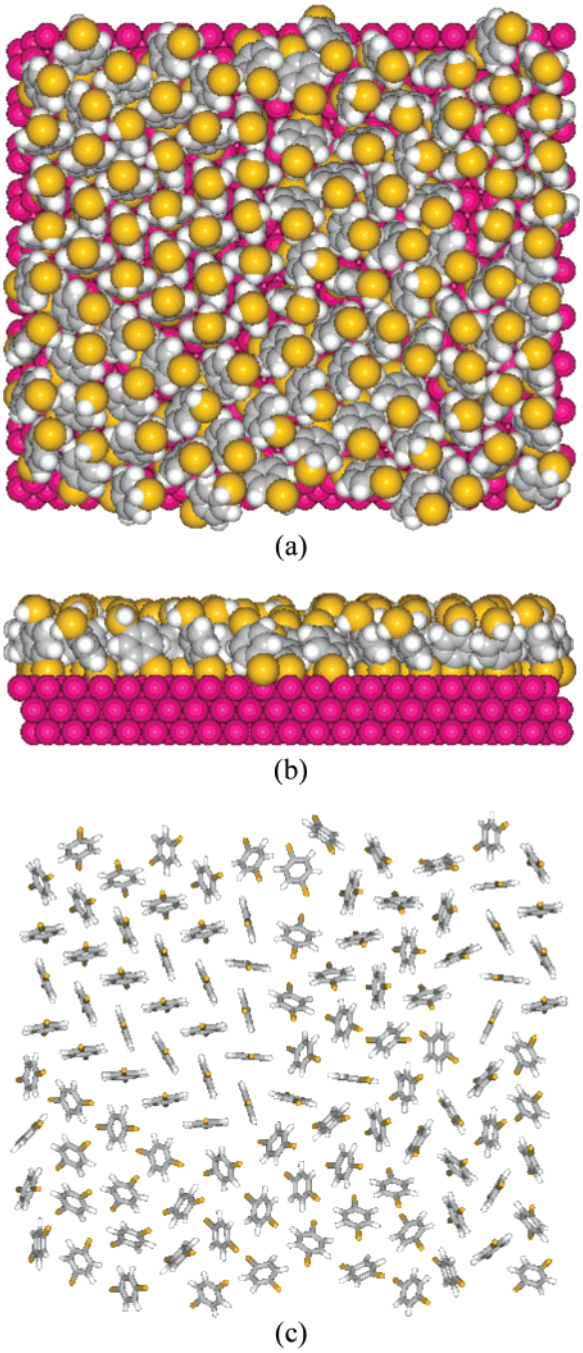

Figure 8. Snapshots of BDT adsorbed on a Au (111) surface with a coverage of $N_a = 6.25\ \mu mol/m^2$ (3.77 molecule/nm^2). (a) Top view, (b) side view, and (c) stick presentation of a.

Table 5. Average Tilting Angles of BDT on Au (111) under Different Coverages

coverage N_a (μmol/m^2)	N_a (molecule/nm^2)	average tilt angle (standard deviation)
0.64	0.38	35°(16°)
1.16	0.70	36°(17°)
2.08	1.26	21°(14°)
2.72	1.64	18°(12°)
4.34	2.61	18°(11°)
6.25	3.77	18°(12°)

of them lie relatively flat. Figure 8 shows only the instantaneous orientations of BDT molecules at certain simulation steps. With the evolution of a simulation run, the orientations of the molecules fluctuate randomly; therefore, the tilting angles can also fluctuate randomly around their average values. In this study, we excluded

(45) Zharnikov, M.; Grunze, M. *J. Phys: Condens. Matter* **2001**, *13*, 11333.
(46) Joo, S. W.; Han, S. W.; Kim, K. *J. Colloid Interface Sci.* **2001**, *240*, 391.
(47) Ehler, T. T.; Malmberg, N.; Noe, L. J. *J. Phys. Chem. B* **1997**, *101*, 1268.
(48) Bubois, L. H.; Zegarski, B. R.; Nuzzo, R. G. *J. Chem. Phys.* **1993**, *98*, 678.
(49) Hautman, J.; Klein, M. L. *J. Chem. Phys.* **1989**, *91*, 4994.
(50) Zarnikov, M.; Frey, S.; Rong, H.; Yang, Y. J.; Heister, K.; Buck, M.; Grunze, M. *Phys. Chem. Chem. Phys.* **2000**, *2*, 3359.

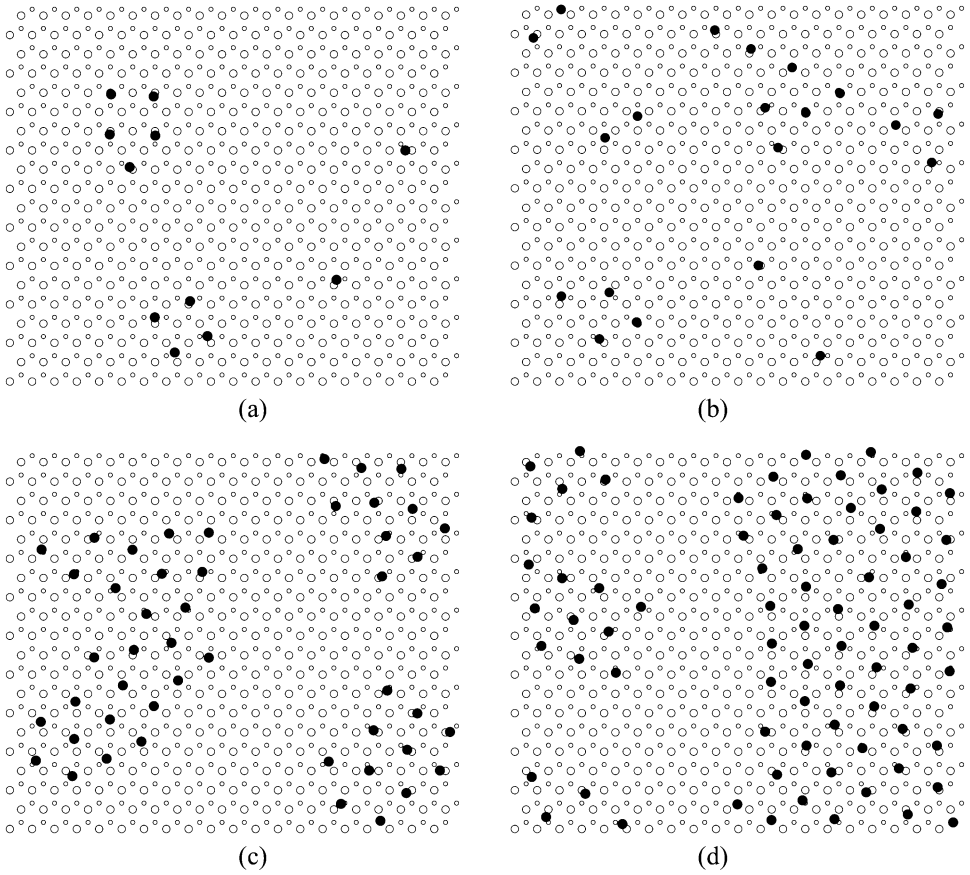

Figure 9. Bonding sites of BDT under different coverages on a Au (111) surface. (a) $N_a = 0.64$ μmol/m^2 (0.385 molecule/nm^2), (b) $N_a = 1.16$ μmol/m^2 (0.70 molecule/nm^2), (c) $N_a = 2.72$ μmol/m^2 (1.64 molecule/nm^2), and (d) $N_a = 4.34$ μmol/m^2 (2.61 molecule/nm^2).

the torsion energy about the C1−S7 and C4−S8 bonds because BDT is considered to be rigid. A previous ab initio calculation study indicates that the rotation barrier of the H−S bond about C−S is only 2.1 kJ/mol, which is comparable to kT at $T = 298$ K.[51] Therefore, we expect that the impact of the exclusion of torsion about C1−S7 (C4−S8) on self-assembly be negligible.

From the snapshots shown in Figures 7 and 8, we can readily conclude that the adsorption of BDT on Au (111) follows a domain growth mechanism, where BDT molecules nucleate around the initial BDT islands. Indeed, by examining snapshots collected at various coverages we find that all of the adsorption followed such a growth pattern (Figure 9). During the first step of adsorption, some BDT molecules stick independently on the Au surface and act as growth centers. Then adsorption takes place with a domain growth pattern. At the same time, the terminal groups of BDT molecules reorient themselves to reach an energy minimum. The kinetics implied in our simulation agrees with the previously reported experimental results on alkanethiols/Au and alkanethiols/Ag systems.[52,53]

The bonding location of alkanethiolate sulfur atoms on the Au surface has been studied by various groups.[11,19,29,44,55] Conclusions from these different studies vary from one another. The consensus, though, is that bonding between the sulfur and gold atoms can occur at any of the following sites: a top site (on a gold atom), a bridge site (between two gold atoms), or a 3-fold hollow site (right in the middle of three gold atoms). However, it is not clear how bonding depends on the adsorption coverage.

Interestingly, we found that the bonding site of BDT sulfur atoms is related to the adsorption coverage. When the coverage is low, the preferable binding sites of BDT molecules on Au (111) are the top sites. As coverage increases, more and more BDT molecules bond on the bridge or hollow sites. Figure 9 shows the most probable bonding sites of BDT molecules on Au (111) at different coverages. The large open circles represent the (x, y) coordinates of Au atoms on the metal surface, and the small open circles represent the second-layer Au atoms. The large filled circles represent the (x, y) locations of sulfur atoms bonded to the Au (111) surface. In this Figure, we present only the 2-D data, and the coordinates in the surface normal direction are not shown. The (x, y) bonding locations in the Figure were calculated by averaging the (x, y) coordinates of bonded sulfur atoms collected during simulations. Please note the data in Figure 9 illustrate the approximate bonding locations of already-adsorbed BDT molecules, which are collected during the *NVT* simulations. They do not represent the adsorption probability of each site accessed by BDT molecules during GCMC equilibration. By simply counting the number of locations that overlap with the top-layer Au atoms, we can estimate the percentage of top site bonding for each coverage. We found that top-site-bonding BDT molecules decreases from more than 80% to about 20% of the total coverage, as the coverage increases from 0.64 μmol/m^2 (0.38 molecule/nm^2) to 4.34 μmol/m^2 (2.61 molecule/nm^2). Further explorations indicate that the percentage of top-site bonding fluctuates around 20% when the coverage is close to full monolayer. From Figure 9, we can also see that adsorbed BDT molecules are strongly trapped and cannot move freely

(51) Wiberg, K. B.; Rablen, R. R. *J. Org. Chem.* **1998**, *63*, 3722.
(52) Himmelhaus, M.; Gauss, I.; Buck, M.; Eisert, F.; Woll, C.; Grunze, M. *J. Electron Spectrosc. Relat. Phenom.* **1998**, *92*, 139.
(53) Bieubyck, H. A.; Bain, C. D.; Whitesides, G. M. *Langmuir* **1994**, *10*, 1825.
(54) Reference deleted in proof.
(55) Camillone, N.; Eisenberger, P.; Leung, T. Y. B.; Schwartz, P.; Scoles, G.; Poirier, G. E.; Tarlov, M. J. *J. Chem. Phys.* **1994**, *12*, 11031.

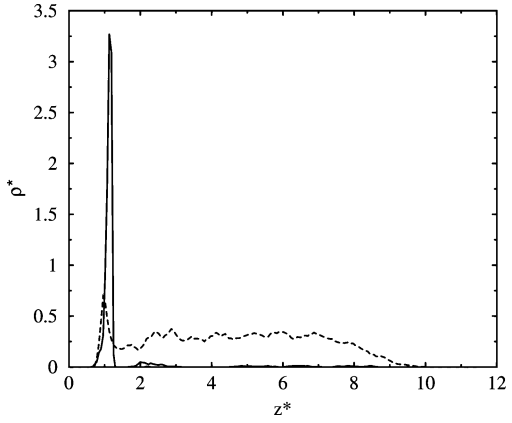

Figure 10. Density profiles of the BDT−THF mixture along the normal direction of Au (111). The solid line is for BDT, and the dashed line is for THF. The coverage of BDT is 5.15 μmol/m^2 (3.10 BDT molecule/nm^2), and the coverage of THF is 20.44 μmol/m^2 (12.31 THF molecule/nm^2).

over the entire surface during *NVT* sampling, although their orientations were observed to fluctuate extensively during the simulation.

For the BDT molecules not adsorbed on top sites, it is sometimes hard to distinguish clearly if they are bonding to a bridge or hollow site (e.g., Figure 9b−d) on the basis of the simulation data collected. However, it is fair to conclude from our simulation results that any of the three sites as reported in experimental studies[55,56] is possible for bonding, but top-site bonding is more favorable at low coverage and hollow and bridge sites are favored at higher coverage.

We attribute the bonding of a BDT molecule to a particular site to the balance between S−Au chemisorption and the physical inter-BDT interactions. The chemical BDT−Au interaction dominates the total system energy, but with increasing coverage, BDT molecules experience more and more interaction from other adjacent BDT molecules. Such inter-BDT interaction may not change the general adsorption nature of the system but could be ineligible in terms of impacting the bonding details of BDT, especially at high coverage. Previous ab initio calculations indicate that the binding energies at the top and the hollow sites are comparable. [11] This seems to suggest that top site and bridge site are equally favorable for BDT molecules to bond. However, we notice that ab initio calculations of SAMs on Au/Ag surfaces focus only on a finite domain because of computational limitations.[11,57,58] Several other studies have been focused on the adsorption energetics of different sites for SAMs similar to the system in this work, but their results were inconsistent with one another.[59−61]

3. BDT−THF Mixture Adsorption. On the basis of the study of bulk BDT and THF adsorption simulations, we have performed BDT−THF mixture adsorption simulation. The coverage of the BDT−THF mixture was achieved using GCMC simulation by adjusting the chemical potentials of BDT and THF components on the basis of the single-component simulations discussed above. The structures of mixture on Au (111) are obtained from *NVT* samplings following the GCMC simulations.

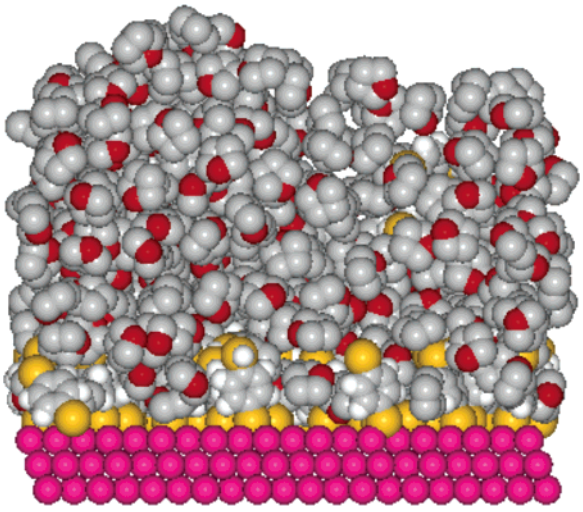

Figure 11. Snapshot of BDT−THF mixture adsorption on Au (111). The mixture coverage is same as that shown in Figure 10.

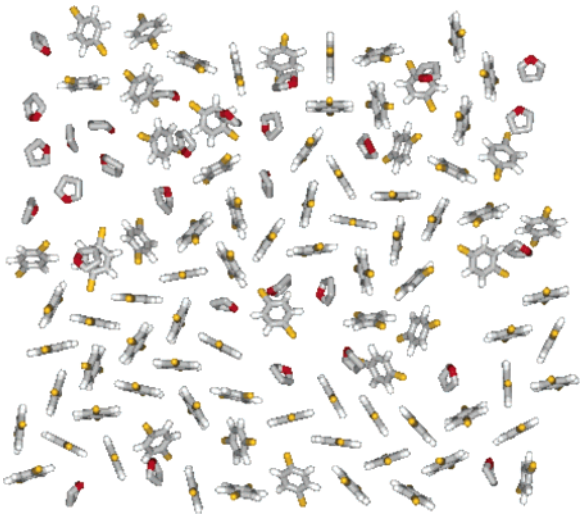

Figure 12. Stick presentation of a mixture monolayer snapshot. The monolayer BDT coverage (excluding the BDT molecules beyond the monolayer) is 4.92 μmol/m^2 (2.96 BDT molecule/nm^2). The total mixture coverage is the same as that in Figure 10. For clarity, only THF and BDT molecules within the monolayer are shown.

Our results indicate that BDT molecules in the mixtures are selectively adsorbed on the Au (111) surface. BDT molecules anchor to the Au (111) surface with one of the sulfur atoms bonded to Au atoms. The solvent THF molecules either float above the BDT monolayer to form amorphous clusters or occupy the vacancy on the Au (111) surface that is not covered with BDT molecules. This is shown by the density profiles of BDT−THF mixtures in Figure 10 and the snapshot in Figure 11. Most of the BDT molecules adsorb and bond on the Au surface (as shown by the sharp peak in Figure 10); a few BDT molecules stay above the chemically bonded BDT monolayer, mixed with the solvent THF molecules.

We found that the presence of solvent THF molecules in the system does not affect the adsorbed structure of BDT significantly. The ordering and structures exhibited by mixture BDT molecules adsorbed on the Au (111) surface is very similar to that of pure BDT adsorbed on Au (111). The monolayer BDT molecules bond to the Au surface with a tilt angle of about 18° at a mixture coverage of 5.15 μmol/m^2 (3.10 BDT molecule/nm^2) BDT and 20.44 μmol/m^2 (12.31 THF molecule/nm^2) THF. In addition, the oriented BDT molecules form a localized herringbone structure

(56) Lee, S. B.; Kim, K.; Kim, M. S.; Oh, W. S.; Lee, Y. S. *J. Mol. Struct.* **1993**, *296*, 5.
(57) Sellers, H.; Ulman, A.; Shnidman, Y.; Eilers, J. E. *J. Am. Chem. Soc.* **1993**, *115*, 9389.
(58) Gronbeck, H.; Curioni, A.; Anderoni, W. *J. Am. Chem. Soc.* **2000**, *122*, 3839.
(59) Bain, C. D.; Troughton, E. B.; Tao, Y. T.; Evall, J.; Whitesides, M.; Nuzzo, R. G. *J. Am. Chem. Soc.* **1989**, *111*, 3221.
(60) Jung, L. S.; Campbell, C. T. *Phys. Rev. Lett.* **2000**, *84*, 5164.
(61) Karpovich, D. S.; Blanchard, G. J. *Langmuir* **1994**, *10*, 3315.

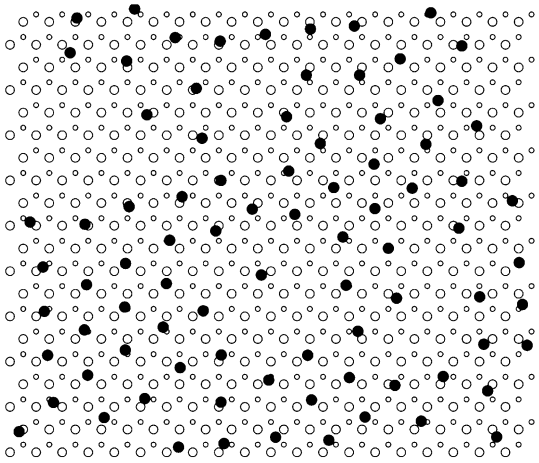

Figure 13. Bonding sites of BDT for BDT−THF mixture adsorption on a Au (111) surface corresponding to the coverages in Figure 12. For clarity, only BDT molecules within the monolayer are shown.

similar to the ones exhibited in pure BDT adsorption (compare Figures 12 and 8c), which is often seen in alkanethiolate SAMs on Au (111).[55,57,62,63] However, we can see that the presence of THF solvent in the system more or less affects the BDT ordering details on Au (111), especially for the BDT molecules on the boundary where some THF molecules occupy the vacancy that is left out. As shown in Figure 12, some BDT molecules do not maintain the tilted orientation when the neighboring molecule(s) is(are) THF. This is probably due to uneven steric effects. As pointed out previously, the uniform steric interactions between BDT adsorbates play a significant role in helping alkanethiolate molecules to form an ordered adsorbate structure.[57]

The bonding sites of BDT on Au (111) for BDT−THF mixture adsorbates are roughly similar to the ones with similar coverage presented in the previous section. For example, the most probable BDT bonding sites for BDT−THF mixture adsorption with coverages of 5.15 μmol/m^2 BDT and 20.44 μmol/m^2 THF are shown in Figure 13. In the Figure, the data for THF and BDT molecules beyond the monolayer are removed for clarity. It can be seen that about 80% of BDT molecules are bonded to bridge or fcc hollow sites, which is comparable to the percentage of pure BDT adsorption on Au (111) with similar coverage. (See Figure 9d for comparison.)

V. Conclusions

In this study, we investigated the adsorption of THF/BDT on the Au (111) surface using Monte Carlo simulations. THF molecules form amorphous clusters on the Au (111) surface rather than spreading out as layers even at very low adsorption coverage. In contrast, BDT molecules form a sharp monolayer on the Au (111) surface. BDT molecules are tilted on average 18 to 35° with respect to the surface normal and form an ordered herringbone structure. The tilting angle decreases slightly with the increase in coverage. The adsorption of BDT on Au (111) follows a domain growth mechanism.

Interestingly, we found that the bonding site of BDT sulfur atoms is dependent on the adsorption coverage. When the coverage is low, the preferable bonding site is the Au top site. With an increase in coverage, more and more BDT bonds on the Au bridge or fcc hollow sites. We attribute this effect to the balance between the S−Au chemical bonding interactions and the interadsorbate interactions.

We have also performed BDT−THF mixture adsorption simulation. Our results indicate that BDT molecules are selectively adsorbed onto the Au (111) surface with one of the sulfur atoms bonded with Au atoms, whereas the solvent THF molecules stay above the BDT monolayer or adsorb onto the Au surface vacancy left out by the BDT molecules. However, the presence of solvent THF in the systems seems not to influence the surface ordering and bonding pattern of BDT on Au (111) appreciably.

Acknowledgment. We acknowledge the financial sponsorship from the Office of Science of the U.S. Department of Energy Computational Nanoscience Project. The computations were performed in the Center for Computational Sciences at Oak Ridge National Laboratory, which is operated by UT-Battelle, LLC under contract no. DE-AC05-00OR22725.

LA0532252

(62) Alves, C. A.; Smith, E. L.; Porter, M. D. *J. Am. Chem. Soc.* **1992**, *114*, 1222.

(63) Alves, C. A.; Porter, M. D. *Langmuir* **1992**, *9*, 3507.